Polymer knot confined in a tube: Statics and relaxation dynamics

Yu-Jane Sheng* and Kuang-Ling Cheng
Department of Chemical Engineering, National Taiwan University, Taipei, Taiwan 106, Republic Of China
(Received 29 May 2001; published 7 December 2001)

The statics and relaxation dynamics of a polymer knot confined in a cylindrical tube of diameter D are investigated by Monte Carlo simulations. The prime knots with crossings varying from 3_1 to 7_1 are considered. The equilibrium radius of gyration along the axial direction is scaled as $R_\parallel \sim R_F(R_F/D)^m$, where R_F is the Flory radius of a knotted polymer. Our simulation results suggest that $m=0.95$, which is different from the value for a linear chain, $m=2/3$. The relaxation behavior of the knotted polymer is studied after the tubular constraint is removed. The relaxation time can be scaled as $\tau_\parallel \sim N R_F^{1+1/m} R_\parallel^{1-1/m}$, which is confirmed by simulations. The effect of topological complexity on both properties is manifested through the Flory radius.

DOI: 10.1103/PhysRevE.65.011801 PACS number(s): 61.41.+e, 83.10.Rs, 87.10.+e

I. INTRODUCTION

The study of the static and dynamic properties of a polymer chain is the key to the understanding of many polymeric materials. With the great improvements in experimental techniques, it is now possible for experimentalists to manipulate a single polymeric molecule, such as a DNA molecule, under desired conditions and to observe the changes in static and dynamic behaviors. For example, Perkins and co-workers [1,2] were able to stretch a single DNA molecule to full elongation under flows and the relaxation behavior of the chain was observed as the flow stopped. This work inspired much theoretical work in both scaling analysis and computer simulation [3–7] because of its important relation to the fundamentals of polymer physics. Many biological molecules, for instance, DNA, take the form of a knotted ring and there are certain types of enzyme that can act on circular DNA and produce different types of knot [8–10]. The physical properties of knots are strongly affected by their topological properties. Investigation of topological effects on the statics and dynamics of knotted polymers could be important in understanding the behavior of DNA.

De Gennes [11] performed some scaling analysis on the static properties of a linear flexible polymer chain of length N confined within a cylindrical tube of diameter D. Sheng and Wang [12] used the bead-spring chain model in continuous space to explicitly verify the universality of the scaling laws. The nonequilibrium relaxation behaviors were also studied. The simulation results confirm the scaling analysis result that the characteristic relaxation time scales as $\tau_\parallel \sim N^2 D^{1/3}$. In the early stage, the relaxation is primarily due to the movement of the free ends, similar to a stretched linear chain being released from the stretching force. The behavior is also consistent with the prediction of the ''stem and flower'' model proposed by Brochart-Wyart and co-workers [3,4]. At longer times, the whole chain undergoes an exponential relaxation behavior.

Great advances have been made in classifying knots and topological invariants in recent decades [13–16]. Some efforts have been made to relate the topological invariants of knots to the static properties of the knotted polymers [17–21]. Quake [17] expressed the knot complexity in terms of the number of essential crossings C. Grosberg *et al.* [18] introduced another topological invariant p, which is the aspect ratio of the length (L) to the diameter (d) of a knot at its maximum inflated state. A schematic drawing for the definition of p can be seen in Fig. 1 of Ref. [18]. The value of p [19] measures the complexity of a knot and it can distinguish knots somewhat better than C. Following the classical Flory approach, the equilibrium radius of gyration of a knotted polymer can be determined by minimization of the free energy, which consists of elasticity due to entropy and interactions between monomers. The interaction term for the knot is identical to that of a linear chain. The elastic free energy, proposed by Grosberg *et al.*, is equivalent to the entropy of a linear polymer in a straight tube with aspect ratio p and volume R_F^3. The polymer ends are attached to the tube ends. This gives

$$R_F \sim a N^\nu p^{-4/15},$$

where N is the number of monomers in the chain and a is the monomer size. R_F is also called the Flory radius. This expression was confirmed in our previous work [20].

The static properties of a knotted polymer under a stretching force have been studied by the Monte Carlo method [21]. The results indicate that for stretched knots the scaling behaviors are the same as that of a linear chain. However, the elastic modulus of a knotted polymer is larger than that of an equal-length linear chain. The nonequilibrium dynamics of a knotted polymer can also be investigated by cutting a prime knot [20]. The result for the relaxation of a knotted chain into a linear one revealed that even prime knots should be classified into different groups based on their topological similarity.

A closely related topic also concerning the physics of a single polymer chain is the study of a knotted chain molecule under a geometrical constraint. In this paper, both statics and dynamics of a prime knot confined in a cylindrical tube of diameter $D \ll R_F$ are analyzed through Monte Carlo simulations. Noticeably, the physical properties of knotted chains are not only functions of chain length N, but also greatly affected by the topological complexity of different knots

*Corresponding author.

[20,21]. In Sec. II we briefly describe the simulation details for prime knots modeled by beads connected by stiff springs. The parameters are chosen to avoid occurrence of bond crossing within the knotted chain. The ensemble-average radius of gyration along the axis direction, $R_\parallel$, is obtained at equilibrium. On the other hand, when the confinement is removed, the time variation of the radius of gyration is recorded. The characteristic time for relaxation, $\tau_\parallel$, is then determined. In Sec. III simple scaling expressions for both $R_\parallel$ and $\tau_\parallel$ are proposed. The length occupied by a polymer chain in the tube can be scaled as $R_\parallel \cong R_F(R_F/D)^m$. For a linear chain, $m=2/3$. However, for a knotted chain, which possesses a topological effect, m remains unknown and needs to be determined from simulation results. The relaxation time of a prime knot is also discussed using a similar approach.

II. MODEL AND SIMULATION DETAILS

The knotted polymer chain studied in this work is modeled as beads connected by stiff springs. The interactions between the nonbonded beads are through the square-well potentials

$$U_{nb}=\begin{cases}\infty & (\sigma>r)\\ -\varepsilon & (\lambda\sigma>r\geqslant\sigma)\\ 0 & (r\geqslant\lambda\sigma),\end{cases} \tag{1}$$

where ε and σ are the energy and size parameters, respectively, and $\lambda=1.5$. The monomeric ε and σ are the units used for the reduced quantities for temperature and distance as $T^*=kT/\varepsilon$ and $R^*=R/\sigma$. The interactions between bonded beads are represented by a cutoff harmonic spring potential as

$$U_b=\frac{1}{2}k\sigma^2\left(\frac{r}{\sigma}-1.2\right)^2, \quad 1.4\geqslant\frac{r}{\sigma}>1.0. \tag{2}$$

The potential is infinite elsewhere. We have chosen $k\sigma^2/\varepsilon=400$. The parameters in the model are chosen to prevent any bond crossing occurring within the knotted chain.

The systems studied contain a single polymer chain with chain length N ranging from 42 to 120. The simulations are performed under the conditions of constant temperature, volume, and total number of beads. In the present study, the reduced temperature $T^*=10$ is chosen so that the system is in the good solvent regime. We have studied the knotted polymers up to seven crossings: 3_1, 4_1, 5_1, 6_1, and 7_1. The standard notation for uniquely labeling a knot is C_K, where C is the number of essential crossings and K is an index for a particular knot [20,16].

The initial configurations are generated by growing the chain bead by bead to the desired length and knot type. To simulate a single knotted polymer chain confined in a tube of diameter D, we use force to ''drag'' the chain into the tube. The trial moves employed for the equilibration and production processes of chains are bead displacement motions [22], which involve randomly picking a bead and displacing it to a new position in the vicinity of the old position. The distance away from the original position is chosen with a probability such that the condition of equal sampling of all points in the spherical shell surrounding the initial position is satisfied. The interactions between the chain and the tube wall are purely excluded volume. The new configurations resulting from this move are accepted according to the standard Metropolis acceptance criterion [23]. Runs for the same chain length at different tube diameters are performed starting with the final configuration from a previous diameter and are equilibrated for 70×10^6 Monte Carlo steps (MCS). Measurements of static properties such as the radius of gyration along the axial direction are taken over a period of $(5-10)\times10^6$ MCS/monomer.

The mean radii of gyration along the axial and radial directions are given by

$$\langle R_\parallel\rangle=\left\langle\frac{\sum_{i=1}^{N}(z_i-z_{CM})^2}{N}\right\rangle^{1/2}, \tag{3}$$

$$\langle R_{perp}^2\rangle=\left\langle\frac{\sum_{i=1}^{N}[(x_i-x_{CM})^2+(y_i-y_{CM})^2]}{N}\right\rangle, \tag{4}$$

where (x_i,y_i,z_i) are the coordinates of the ith monomer in the chain and (x_{CM},y_{CM},z_{CM}) are the coordinates of the center of mass of the chain. The angular brackets $\langle\ \rangle$ denote the ensemble average.

The nonequilibrium dynamical process of releasing the confinement of the chain at $t=0$ is characterized by the time dependence of the z component of the radius of gyration $R_\parallel(t)$:

$$\frac{\overline{R_\parallel(t)}}{R_\parallel(0)}\sim\exp\left(-\frac{t}{\tau}\right), \tag{5}$$

where $R_\parallel(0)$ is the radius of gyration in the z direction at $t=0$ and to overbar denotes an average over different realizations of the relaxation process. Typically, this average is taken for 500–1500 realizations in our simulations. Time is measured in units of Monte Carlo steps per monomer; 1 MCS/monomer means that on average every monomer has attempted to move once.

III. RESULTS AND DISCUSSION

On the basis of the Monte Carlo scheme, the static and relaxation dynamic properties of a polymer knot confined in a cylindrical tube are calculated for different values of the tube diameter and also for different chain lengths. In this section scaling expressions for the radius of gyration and the relaxation time are proposed and verified by simulations.

A. Static properties

As mentioned in Sec. I, de Gennes [11] performed a scaling analysis and obtained scaling laws for the static properties of a single polymer chain confined in a cylindrical tube

of diameter D. The system has two characteristic lengths, the diameter of the tube and the Flory radius $R_F = aN^{\nu}$, where N is the number of monomers in the chain and a is the monomer size. In good solvent conditions, $\nu \approx 3/5$. Under the conditions $a \ll D \ll R_F$, the chain can experience confinement but can still wiggle in the lateral direction. The length occupied by the chain in the tube $R_\parallel$ has the scaling form

$$R_\parallel = R_F \Phi_\parallel \left(\frac{R_F}{D} \right), \tag{6}$$

where $\Phi_\parallel(x)$ is a dimensionless scaling function. For a thick tube, i.e., $D \gg R_F$, since the wall of the tube has little effect on the chain, we expect $R_\parallel$ to be approximately proportional to R_F, that is, $\Phi_\parallel(x) \to 1$ for $x \to 0$. For a thin tube where $D \ll R_F$ (i.e., $x \to \infty$), $\Phi_\parallel(x)$ is assumed to be proportional to x^m. Since the chain becomes a one-dimensional chain for a thin tube, one anticipates that $R_\parallel$ must be linear in N, $R_\parallel \equiv aN^{\nu}(aN^{\nu}/D)^m \sim N$. As a consequence, $m = 1/\nu - 1$ and $m = 2/3$ in the good solvent regime. This result has been confirmed by Monte Carlo simulations in our previous work [12]. The chain length along the tube can then be expressed as $R_\parallel = Na(a/D)^{1/\nu - 1} \sim ND^{2/3}$.

One would expect that the situation for a polymer knot confined within a tube is somewhat like that for a linear chain. Nevertheless, the topological effect associated with knots comes into play. The system possesses two characteristic lengths as well; that is, the tube diameter D and the Flory radius R_F of the knot. According to the scaling by Grosberg *et al.* [18], the radius of a gyration of a knotted polymer in a good solvent is scaled as $R_F \sim N^{\nu} p^{-4/15}$, where p brings in the topological effects on a knotted type polymer. The value of p increases as the complexity of the knot increases. For example, $p = 16.4$, 21.2, 24.2, 29.3, and 30.9 for 3_1, 4_1, 5_1, 6_1, and 7_1 [19], respectively. In accord with the Buckingham Π theorem, the length occupied by the chain in the tube $R_\parallel$ should also have the scaling form $R_\parallel = R_F \Phi_\parallel(R_F/D)$. Similar to a linear chain, the knotted polymer inside a thick tube can retain its conformation without being significantly affected by the wall of the tube. Thus, $\Phi_\parallel(R_F/D) \to 1$ for $R_F/D \to 0$. Inside a thin tube, $\Phi_\parallel(R_F/D)$ can also be assumed to be proportional to $(R_F/D)^m$. Although a linear chain in a thin tube is allowed to be stretched like a one-dimensional string, a knotted polymer possesses conformations of loops and has several numbers of crossings within the loop. The significance of the topological effects is yet to be explored and therefore m can be determined only by results of simulations or experiments. Under the condition of $D \ll R_F$, whether the knotted polymer displays a one-dimensional structure or not becomes an interesting question. The outcome may shed some light on the topological interactions between the knot and the tube.

Since the topological effect on the confined knotted chain is unknown, we first perform simulations in continuous space to investigate the static structure and make an attempt to find the scaling relation. Figure 1 demonstrates snapshots of a polymer knot 4_1 with length $N = 82$ confined within a tube at different diameters (D) scaled by a. When D is approximately equal to R_F, the interactions between the chain beads and the tube wall are insignificant and the chain can roughly retain its constant Flory coil formation even within the tube. When D is apparently smaller than R_F, the excluded volume interactions between the knot and tube wall become substantial and prevent the knot from maintaining the Flory coil conformation. The degree of extension in the axial direction is increased with decreasing D. Note that a linear chain can be compressed into a tube with $D \approx a$. The chain becomes almost fully extended in response to such compression. However, a knotted chain has intrinsic constraints to prevent it from being extended in a linear fashion. As shown in Fig. 1, this prime knot (4_1) can be compressed only into a tube of diameter about $D \approx 5$.

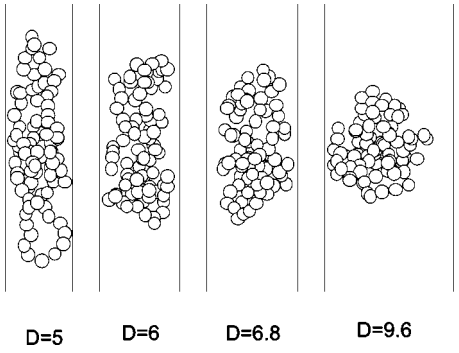

FIG. 1. Snapshots of a knotted chain 4_1 with length $N = 82$ confined within a tube at different diameters (D) scaled by a. The bead diameter has been decreased for the purpose of clarity.

Figure 2 shows the results of the Monte Carlo simulations for 3_1 and 6_1 knots of different chain lengths trapped within tubes of different diameters in the good solvent regime. The $R_\parallel$ is plotted against $D/2$ on a log-log plot. On average, the best fit linear lines yield a value of slope ≈ -0.95. This result indicates that the scaling law for $R_\parallel$ takes the following form:

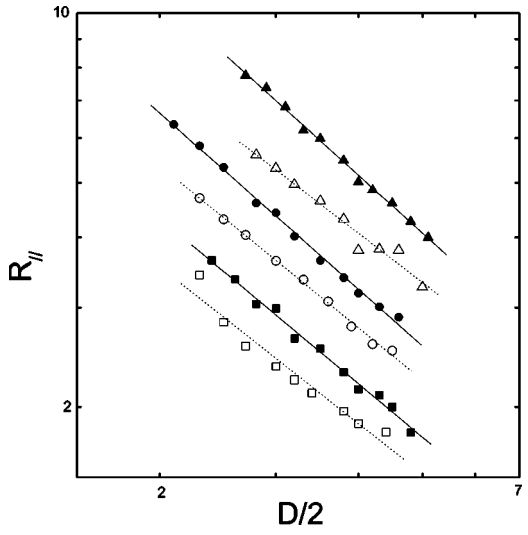

FIG. 2. The mean radius of gyration in the axial direction $R_\parallel$ vs the radius of the tube $D/2$ for two types of knot at various chain lengths. 3_1: (□) $N = 42$; (○) $N = 60$; (△*up*) $N = 82$. 6_1: (■) $N = 60$; (●) $N = 82$; (▲) $N = 120$. The dotted and solid lines are the best-fitted curves for the 3_1 and 6_1 knots, respectively.

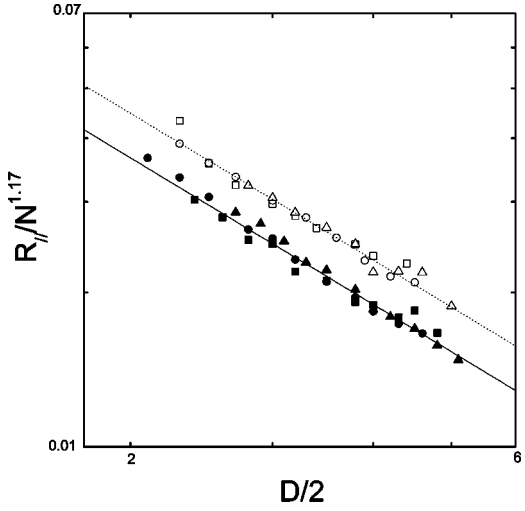

FIG. 3. The scaled mean radius of gyration in the axial direction $R_{\parallel}/N^{1.17}$ vs the radius of the tube $D/2$ for two types of knot at various chain lengths. 3_1: (□) $N=42$; (○) $N=60$; (△*up*) $N=82$. 6_1: (■) $N=60$; (●) $N=82$; (▲) $N=120$. The dotted and solid lines are the scaling curves for the 3_1 and 6_1 knots with slope of -0.95.

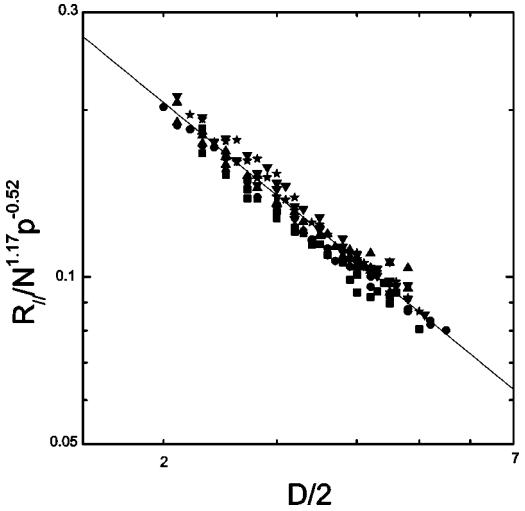

FIG. 4. The scaled mean radius of gyration in the axial direction $R_{\parallel}/N^{1.17}p^{-0.52}$ vs the radius of the tube $D/2$ for five types of knot at various chain lengths. 3_1: (■) $N=42$, $N=60$, and $N=82$. 4_1: (●) $N=42$, $N=60$, and $N=82$. 5_1: (▲) $N=42$, and $N=60$, and $N=82$. 6_1: (▼) $N=60$, $N=82$, and $N=120$. 7_1: (⋆) $N=60$, $N=82$, and $N=120$. The solid line is the scaling curve with slope of -0.95.

$$R_{\parallel}\sim R_F\left(\frac{R_F}{D}\right)^{0.95}. \tag{7}$$

Equation (7) can be expressed in terms of p for $\nu\approx 0.6$,

$$R_{\parallel}\sim N^{1.17}p^{-0.52}D^{-0.95}. \tag{8}$$

Note that this scaling relation is quite different from the one-dimensional chain argument for the linear chain, which gives $R_{\parallel}\sim ND^{-2/3}$. $R_{\parallel}$ of a knotted chain has a stronger dependence on D than that of a linear chain. This fact implies that the loops within a knot being forbidden to cross one another enhances the excluded interactions between the knotted chain and the wall. To further verify the relation, we have plotted $R_{\parallel}/N^{1.17}$ against $D/2$ on a log-log plot. As one can see from Fig. 3, data for knots 3_1 and 6_1 with different chain lengths collapse into two separate lines. This result shows that the scaling relation $R_{\parallel}\sim N^{1.17}$ is also valid. The difference between these two data sets comes from the topological effects of the two different types of knot. Finally, as depicted in Fig. 4, we have taken into account the effects of chain lengths (N) and knot complexity (p) on $R_{\parallel}$ and all the data for different knots with different collapse crumple together. The best-fitted line for these data has a slope approximately equal to -0.93. Again, the results verify the validity of Eq. (8).

Note that $R_{\parallel}$ is proportional to N^{α} where $\alpha\approx 1.17$. We are aware of the fact that for a linear chain $\alpha\ \nu(\approx 0.6)$ for $D\gg R_F$ and becomes 1 as $D\ll R_F$. On the basis of this conclusion, one would intuitively anticipate that it is impossible for the exponent α to be greater than 1. In this study, however, α is found to be greater than 1 for a knotted chain. As described in the previous section, the exponent m is first obtained from the simulation results for $R_{\parallel}$ and D combined with the well-known dependence of R_F on N [18,20]. Then, with the chain length altered directly, the data of $R_{\parallel}/N^{\alpha}$ against D collapse into one line and thus confirm the prediction. We therefore believe that the simulations are self-consistent and a scaling law with insight into physics is worthy of further pursuit. A possible explanation is that the knotted chain in this study is in an intermediate regime between a free chain and a completely stretched chain. The power law is still followed in this regime, arising from the competition between the external, geometrical constraint and the internal topological effect inherent in the knot.

We have also recorded the lateral spread of the chain $\langle R_{perp}^2\rangle$ for different chain lengths and types of knot. The variation of $\ln\langle R_{perp}^2\rangle$ with $\ln(D/2)$ is plotted in Fig. 5. A fairly good linear relation between $\langle R_{perp}^2\rangle$ and D^2 is shown and therefore $\langle R_{perp}^2\rangle$ scales as D^2 for $D\ll R_F$, as expected. The deviation from the linear relation for large values of D indicates that for $D\gtrsim 2R_F$ a transition takes place. The characteristic volume associated with a confined chain can be estimated as $V\sim R_{perp}^2 R_{\parallel}$. Consequently, one has $V\sim D^{4/3}$ for a linear chain. For a knotted chain, however, $V\sim D^{2-m}\approx D^{1.05}$. Due to the looped structure, the volume of the confined knot increases with increasing D less evidently than that of a linear chain.

B. Dynamic properties

We have studied the static properties of a polymer knot initially confined in a tube and allowed to equilibrate within the tube. In this work we are also interested in the nonequilibrium relaxation behavior, after the constraint is removed. Recall that the confinement energy of a linear chain confined in a tube, according to de Gennes [11], can be expressed as

$$F_{conf}\cong T\phi\left(\frac{R_F}{D}\right). \tag{9}$$

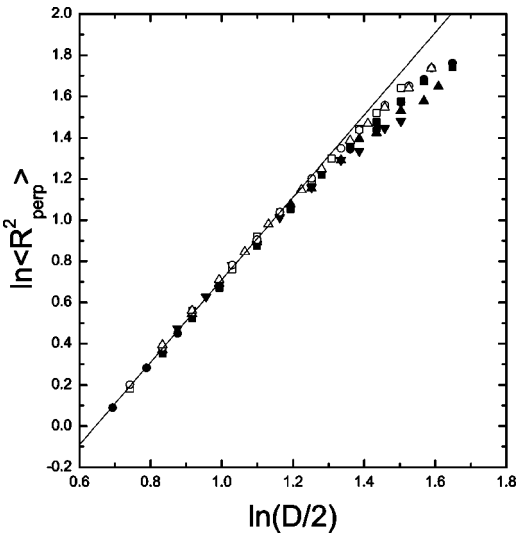

FIG. 5. The variation of the lateral spread $\ln\langle R_{perp}^2\rangle$ of knots as a function of $\ln(D/2)$ for various knots. (■) 3_1, $N=60$; (●) 4_1, $N=60$; (▲) 5_1, $N=60$; (▼) 6_1, $N=60$; (□) 5_1, $N=82$; (○) 6_1, $N=82$; (△*up*) 7_1, $N=82$. The solid line is the scaling curve with slope of 2.

In the strong confinement limit, $D \ll R_F$ (i.e., $R_F/D \to \infty$), the energy has a linear relation with N, $F_{conf} \cong T(R_F/D)^x \sim N$. Consequently, $x=1/\nu$ and $F_{conf}=TN(a/D)^{1/\nu}$. The foregoing equation can be rearranged to give $F_{conf} \cong T(R_\parallel/R_F)^{1/(1-\nu)}$, where $R_\parallel = Na(a/D)^{1/\nu-1}$. For a polymer knot confined within a tube, however, $R_\parallel$ is not proportional to N in the limit of $R_F \gg D$. $R_\parallel$ is proportional to $N^{1.17}$ instead. It is reasonable to speculate that the confinement energy in the present case does not have a linear relation with N. In light of the blob theory, the polymer knot can be assumed to break up into an ideal string of noninteracting blobs, each with size D. This scenario is valid when the resulting knot extension exceeds the Flory radius R_F but is not yet comparable to the fully extended length under external confinement. The blob size is related to the effective stretching force and temperature via $D=k_BT/f_{eff}$, where k_B is the Boltzmann factor. Thus, $f_{eff}=(k_BT/R_F)(R_\parallel/R_F)^{1/m}$ and the confinement energy of the knot is equivalent to the elastic work done by the effective stretching force. The work can then be estimated as

$$W_{el} = \int_0^{R_0} f_{eff} dR_\parallel \sim k_B T \left(\frac{R_0}{R_F}\right)^{(1+m)/m}, \tag{10}$$

where $R_0 = R_\parallel(t=0)$.

We attempt to analyze such a relaxation phenomenon by a similar method to that adopted in Ref. [12]. We assume that the confinement energy is dissipated by the viscous damping force after the constraint imposed upon the chain is relieved. In our Monte Carlo simulation, there is no hydrodynamic interaction, and therefore the Rouse model is expected to be correct. By using Stokes law, the viscous damping force can be obtained as

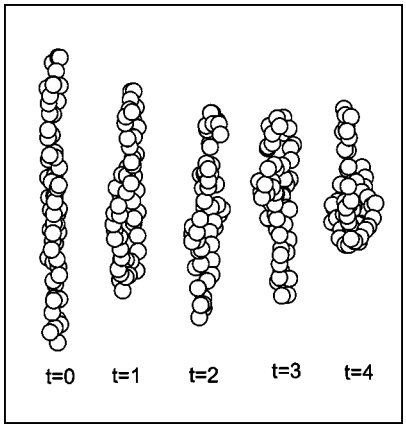

FIG. 6. Snapshots of the configurations of a single knotted chain (4_1,$N=60$) during the relaxation process. Initially, the chain is extended due to the confinement in a tube at $D/2=2.0$. The tube is removed at $t=0$. Snapshots between t and $t+1$ contain 4×10^5 MC steps. The bead diameter has been decreased for the purpose of clarity.

$$f_v = 6\pi\mu a \left(\frac{\partial R_\parallel}{\partial t}\right) N, \tag{11}$$

where μ is the viscosity. Assuming that the relaxation time is dominated by a single time scale $\tau_\parallel$, the time dependence of $R_\parallel(t)$ can be written as $R_\parallel(t)=R_\parallel(0)F(t/\tau_\parallel)$ for some function F. The work dissipated is then given by

$$W_v = \int_0^{R_0} f_v dR_\parallel . \tag{12}$$

Equating Eqs. (10) and (12), $\tau_\parallel$ can be estimated by

$$\tau_\parallel \sim \frac{\mu a}{T} N R_F^{(m+1)/m} R_0^{(m-1)/m} . \tag{13}$$

We have used the relation

$$R_0 = R_F \left(\frac{R_F}{D}\right)^m , \tag{14}$$

where $m=0.95$ and $R_F \sim aN^\nu p^{-4/15}$. In good solvents, $\nu \approx 0.6$, one obtains the relaxation time from Eq. (13),

$$\tau_\parallel \sim N^{2.2} p^{-0.52} D^{0.05}. \tag{15}$$

When the tube is removed at $t=0$, the knotted chain starts to relax toward Flory coil conformation. Figure 6 depicts the relaxation process. One unit of time contains 4×10^5 MC steps. It was found that the relaxation mechanisms are somewhat different from those associated with a linear chain. Owing to the excluded volume interactions between the chain beads and the wall, a linear chain confined in a tube becomes extended. When the constraint is removed, the large-scale relaxation proceeds primarily through the end beads of the chain. For knotted chains, due to the looped structure, there are no free end beads and the relaxation can start only with small-scale internal relaxation by each bead on the chain.

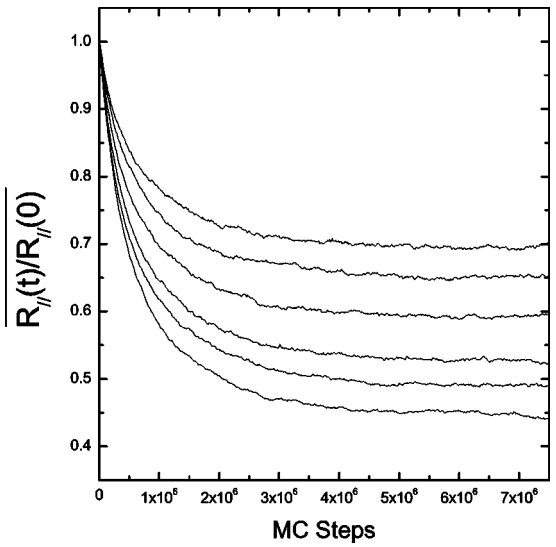

FIG. 7. $\overline{R_{\parallel}(t)/R_{\parallel}(0)}$ for 5_1 and $N=60$ at different diameters of the tube (t in units of MCS). $D/2=2.3$, 2.5, 2.7, 3.0, 3.3, and 3.5 from bottom to top.

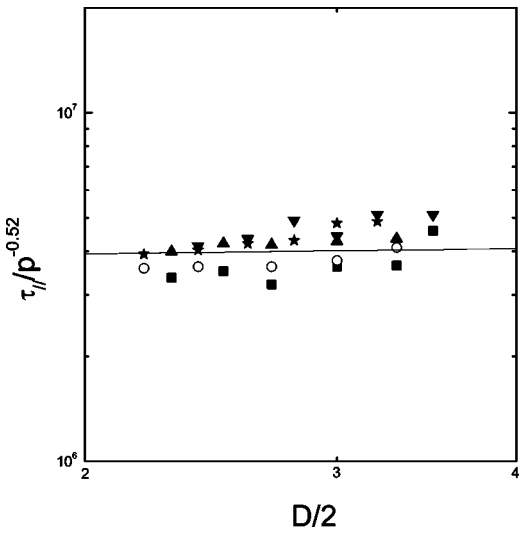

FIG. 9. Monte Carlo data for the relaxation time (in units of MCS/monomer) $\tau_{\parallel}/p^{-0.52}$ vs $D/2$ for various knots at $N=60$: (■) 3_1; (○) 4_1; (▲) 5_1; (▼) 6_1; (⋆) 7_1. The solid line represents the scaling relation with a slope of 0.05.

The conformations of the knotted chains can be probed by looking at snapshots of the relaxation process as shown in Fig. 6. Initially, the knot is in its extended state. As the constraint is removed, the knot starts to recoil. Because of the looped structure of a knotted chain, the relaxation in $R_{\parallel}(t)$ is less evident than that of a linear chain [12]. At $t=4$ (i.e., after 1.6×10^6 steps), the knot approaches its natural state fairly closely.

We have monitored the changes of $R_{\parallel}(t)$ as a function of t, after the constraint is removed, through dynamic Monte Carlo simulations. Figure 7 displays the variation of $\overline{R_{\parallel}(t)/R_{\parallel}(0)}$ versus t for 5_1 and $N=60$ at different tube diameters. Note that, in fact, the radius of gyration of the chain in the z direction fluctuates (as can be seen in Fig. 6 as well). However, the average over many relaxation processes results in a smoothly decaying curve. Those curves in Fig. 7 show the evolution of the ensemble-averaged relaxation processes. In general, these curves are noisier than those for a linear chain. Thus, more realizations of the relaxation process are needed in this study.

The relaxation time $\tau_{\parallel}$ is extracted from the data of $\overline{R_{\parallel}(t)/R_{\parallel}(0)}$ by assuming that it decays exponentially to $R_{\parallel}(\infty)/R_{\parallel}(0)$ as $e^{-t/\tau_{\parallel}}$. Figure 8 shows the variation of $\tau_{\parallel}$ with $D/2$ for 3_1 with $N=42$, 60, and 80. In accord with Eq. (15), it is not surprising that the relaxation time is a fairly weak function of the tube diameter. The lines plotted in

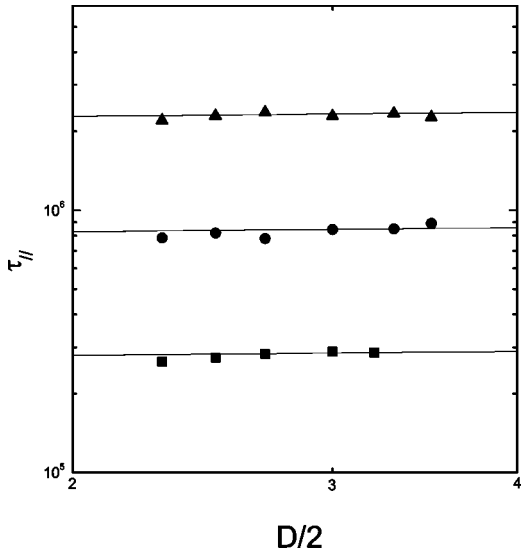

FIG. 8. Monte Carlo data for the relaxation time (in units of MCS/monomer) $\tau_{\parallel}$ vs $D/2$ for 3_1 knot at various chain lengths: (■) $N=42$; (●) $N=60$; (▲) $N=82$. The solid lines are the scaling relation with a slope of 0.05.

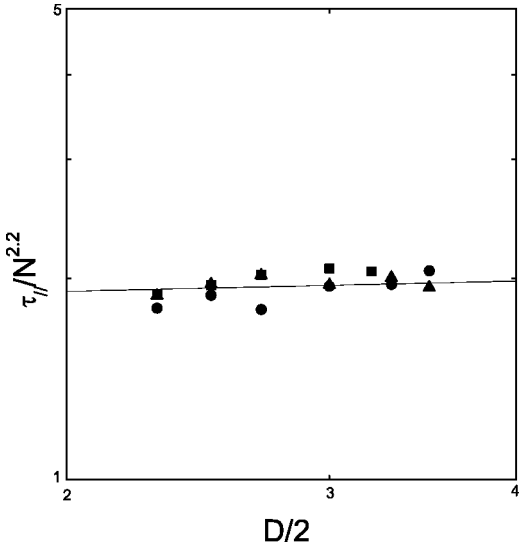

FIG. 10. Monte Carlo data for the relaxation time (in units of MCS/monomer) $\tau_{\parallel}/N^{2.2}$ vs $D/2$ for 3_1 knot at various chain lengths: (■) $N=42$; (●) $N=60$; (▲) $N=82$. The solid line denotes the scaling relation with a slope of 0.05.

Fig. 8 are straight lines with slopes equal to 0.05. The simulation results are quite consistent with our scaling analysis. This result indicates that the chain takes about the same time to relax for various D. This consequence is different from what we observed for a linear chain. We speculate that the relaxation process of a knot consists of two different time-scale regimes. In the early stage, the relaxation is primarily caused by the rearrangement of the ''blobs'' formed within the knot. At longer times, however, the whole chain undergoes relaxation through the movements of each bead. At this stage, the tension of the chain caused by the constraint of the tube wall is relieved and the topological complexity of the knot p has more profound effects on the relaxation process than does D. Thus, $\tau_{\|}$ becomes essentially independent of D.

According to the scaling analysis, we should observe $\tau_{\|} \sim p^{-0.52}$. In Fig. 9, the quantity $\tau_{\|}/p^{-0.52}$ is plotted against $D/2$ on a log-log plot for different types of knot with $N=60$. Although the data are quite scattered, they still exhibit a fairly collapsed pattern. Finally, Fig. 10 illustrates the effect of chain length. The relaxation time $\tau_{\|}$ is scaled with $N^{2.2}$ for 3_1 and $N=42$, 60, and 82. Similarly, the data collapse into a single line with a slope equal to 0.05. The scaling relation $\tau_{\|} \sim N^{2.2}$ is therefore verified.

In this paper, the dynamic Monte Carlo method is adopted to study the relaxation of a knotted chain. In terms of long term, large-scale properties, it is equivalent to the Rouse model, in which the effects of internal friction are negligible [24]. There is another dynamic algorithm that could be used to model a hard-core chain confined to a tube [25,26]. The Brownian dynamics algorithm, with random thermal forces acting on monomers and hydrodynamic interactions neglected, should be capable of reproducing the work presented here.

ACKNOWLEDGMENTS

This research was supported by National Council of Science of Taiwan under Grant No. NSC 90-2214-E-002-016. Y.J.S. would like to thank Professor Heng-Kwong Tsao for helpful discussions. Computing time provided by the National Center for High-Performance Computing of Taiwan is gratefully acknowledged.

[1] T.T. Perkins, S.T. Quake, D.E. Smith, and S. Chu, Science **264**, 822 (1994).
[2] T.T. Perkins, D.E. Smith, R.G. Larson, and S. Chu, Science **268**, 83 (1995).
[3] F. Brochard-Wyart, H. Hervet, and P. Pincus, Europhys. Lett. **26**, 511 (1994).
[4] F. Brochard-Wyart, Europhys. Lett. **30**, 387 (1995).
[5] P.-Y. Lai, Physica A **221**, 233 (1995).
[6] P.-Y. Lai, Phys. Rev. E **53**, 3819 (1996).
[7] Y.-J. Sheng, P.-Y. Lai, and H.-K. Tsao, Phys. Rev. E **56**, 1900 (1997).
[8] W.R. Bauer, F.H.C. Crick, and J.H. White, Sci. Am. **243**, 118 (1980).
[9] N.R. Cozzarelli, S.J. Spengler, and A. Stasiak, Cell **42**, 325 (1985).
[10] S.A. Wasswеman and N.R. Cozzarelli, Science **232**, 951 (1986).
[11] P.G. de Gennes, *Scaling Concepts in Polymer Physics* (Cornell University Press, Ithaca, NY, 1979).
[12] Y.-J. Sheng and M.-C. Wang, J. Chem. Phys. **114**, 4724 (2001).
[13] V.F.R. Jones, Bull. Am. Math. Soc. **12**, 103 (1985).
[14] F.Y. Wu, Rev. Mod. Phys. **64**, 1099 (1992).
[15] L.H. Kauffman, *Knots and Physics*, 2nd ed. (World Scientific, Singapore, 1993).
[16] G. Burde and H. Zieschang, *Knots* (de Gruyter, Berlin, 1985).
[17] S.R. Quake, Phys. Rev. Lett. **73**, 3317 (1994).
[18] A.Yu. Grosberg, A. Feigel, and Y. Rabin, Phys. Rev. E **54**, 6618 (1996).
[19] V. Katritch, J. Bednar, D. Michoud, R.G. Scharein, J. Dubochet, and A. Stasiak, Nature (London) **384**, 142 (1996).
[20] Y.-J. Sheng, P.-Y. Lai, and H.-K. Tsao, Phys. Rev. E **58**, R1222 (1998).
[21] Y.-J. Sheng, P.-Y. Lai, and H.-K. Tsao, Phys. Rev. E **61**, 2895 (2000).
[22] Y.-J. Sheng, A.Z. Panagiotopoulos, S.K. Kumar, and I. Szleifer, Macromolecules **27**, 400 (1994).
[23] M.P. Allen and D.J. Tildesley, *Computer Simulations of Liquids* (Oxford University Press, New York, 1987).
[24] A.Y. Grosberg and A.R. Khokhlov, *Statistical Physics of Macromolecules* (AIP, Woodbury, NY, 1994).
[25] J.M. Deutsch, Science **240**, 922 (1988).
[26] J.M. Deutsch and T.L. Madden, J. Chem. Phys. **90**, 2476 (1989).